

Article

Not peer-reviewed version

# The diagnostic accuracy of artificial intelligence in radiological markers of normal pressure hydrocephalus (NPH) on non-contrast CT scan of the brain

[Akara Supratak](#)<sup>\*</sup>, Dittapong Songsaeng, Poonsuta Nava-apisak, Jittsupa Wongsripuemtet, Siripra Kingchan, [Phuriwat Angkoondittaphong](#), [Phattaranan Phawaphutanon](#)

Posted Date: 22 June 2023

doi: 10.20944/preprints202306.1627.v1

Keywords: NPH; radiologic markers; hydrocephalus; AI



Preprints.org is a free multidiscipline platform providing preprint service that is dedicated to making early versions of research outputs permanently available and citable. Preprints posted at Preprints.org appear in Web of Science, Crossref, Google Scholar, Scilit, Europe PMC.

Copyright: This is an open access article distributed under the Creative Commons Attribution License which permits unrestricted use, distribution, and reproduction in any medium, provided the original work is properly cited.

---

*Article*

# The diagnostic accuracy of artificial intelligence in radiological markers of normal pressure hydrocephalus (NPH) on non-contrast CT scan of the brain

Dittapong Songsaeng <sup>1</sup>, Poonsuta Nava-apisak <sup>1</sup>, Jittsupa Wongsripuemtet <sup>1</sup>, Siripra Kingchan <sup>2</sup>, Phuriwat Angkoondittaphong <sup>2</sup>, Phattaranan Phawaphutanon<sup>1</sup> and Akara Supratak <sup>2,\*</sup>

<sup>1</sup> Department of Radiology, Faculty of Medicine Siriraj Hospital, Mahidol University, Bangkok, Thailand.;

<sup>2</sup> Faculty of Information and Communication Technology, Mahidol University, Salaya, Nakhon Pathom, Thailand.;

\* Correspondence: Akara Supratak Tel:+66(02) 441-0909; akara.sup@mahidol.edu

**Abstract:** Diagnosing Normal Pressure Hydrocephalus (NPH) via non-contrast computed tomography (CT) brain scans is presently a formidable task due to the lack of universally agreed-upon standards for radiographic parameter measurement. A variety of radiological parameters, such as Evans' index, narrow sulci at high parietal convexity, Sylvian fissures' dilation, focally enlarged sulci, and more, are currently measured by radiologists. This study aimed to enhance NPH diagnosis by comparing the accuracy, sensitivity, specificity, and predictive values of radiological parameters, as evaluated by radiologists and AI methods utilizing cerebrospinal fluid volumetry. Results revealed a sensitivity of 77.14% for radiologists and 99.05% for AI, with specificities of 98.21% and 57.14%, respectively, in diagnosing NPH. Radiologists demonstrated NPV, PPV, and accuracy of 82.09%, 97.59%, and 88.02%, while AI reported 98.46%, 68.42%, and 77.42%. ROC curves exhibited an area under the curve of 0.954 for radiologists and 0.784 for AI, signifying the diagnostic index for NPH. In conclusion, although radiologists exhibited superior sensitivity, specificity, and accuracy in diagnosing NPH, AI served as an effective initial screening mechanism for potential NPH cases, potentially easing the radiologists' burden. Given ongoing AI advancements, it's plausible that AI could eventually match or exceed radiologists' diagnostic prowess in identifying hydrocephalus.

**Keywords:** NPH; radiologic markers; hydrocephalus; AI

---

## 1. Introduction

Hydrocephalus is a condition where there is an abnormal accumulation of cerebrospinal fluid (CSF) within the brain's ventricles, resulting in increased intracranial pressure. It is classified into two types; obstructive hydrocephalus, which occurs when there is a physical blockage in the cerebrospinal fluid (CSF) flow pathway, and communicating hydrocephalus, which is characterized by abnormal CSF accumulation in the ventricles and subarachnoid spaces due to defects in reabsorption. Normal pressure hydrocephalus (NPH) is a subtype of communicating hydrocephalus which typically seen in older adults and can present with symptoms such as gait disturbance, urinary incontinence, and memory impairment. These symptoms can be mistaken for Alzheimer's disease or other types of dementia, making NPH a challenging diagnosis [1].

NPH is categorized into two types. The first is idiopathic NPH (iNPH) which is caused by an unknown reason that affects the reabsorption of cerebrospinal fluid back into the

venous system. The second type is secondary NPH which results from various factors such as bleeding in the brain's cerebrospinal fluid, head trauma, infection, tumor, or complications of surgery. These factors can cause the accumulation of cerebrospinal fluid in the brain's ventricles and subarachnoid spaces, leading to NPH symptoms such as gait disturbance, urinary incontinence, and memory impairment.

Several studies have investigated the use of radiological parameters from non-contrast computed tomography (NCCT) of the brain for the diagnosis of hydrocephalus. Nevertheless, diagnosing NPH based on radiographic imaging remains challenging due to the lack of standardized measurement methods for these radiographic parameters [2]. Various radiological parameters which are used to diagnose NPH in our study included Evans' index, narrow sulci at high parietal convexity, dilatation of the Sylvian fissures, focally enlarged sulci, widening of temporal horns, callosal angle, and periventricular hypodensities [3].

With the increasing application of technology in the medical field, artificial intelligence (AI) has emerged as a promising tool for improving diagnostic accuracy and reducing errors in radiology. AI can quickly analyze large amounts of medical data, such as imaging studies, and identify abnormalities that might be missed by human radiologists. By utilizing deep learning algorithms, AI can recognize patterns and anomalies in medical images, providing more accurate and efficient diagnoses [4].

Siriraj Hospital, Mahidol University is utilizing AI innovations for screening pulmonary tuberculosis in chest radiographs and ASPECT in patients with clinical suspected acute cerebrovascular ischemia. Currently, the hospital is conducting research to compare the sensitivity, specificity, positive predictive value, negative predictive value, and accuracy of AI to radiological parameters measured by radiologists in normal and NPH diagnosed groups.

## 2. Materials and Methods

### Patient selection

A retrospective study carried out between December 2012 and August 2022, which included all patients over the age of 18 who had both clinical data and imaging available. NPH was confirmed in patients by the gold standard method for diagnosis, cerebrospinal fluid (CSF) tap test. Patients with intracranial mass, cerebral hemorrhage, and large cerebral infarction leading to anatomical distortion of the brain were excluded from the study.

### Imaging review

CT imaging was assessed for all patients at the time of initial diagnosis. The images were reviewed by two senior neuroradiologists with more than 20 and 10 years of working experience and a third-year radiology resident, who were blinded to the patients' clinical status, using the department Picture Archiving and Communication System (PACS). Inter-observer agreement was evaluated between the two neuroradiologists and the resident. In cases of disagreement, the final judgement, were made by consensus. The AI was also used to evaluate the same groups of patients and identify cases of NPH.





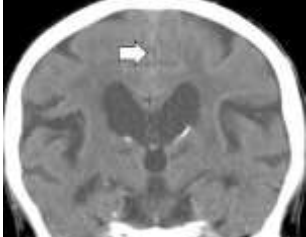


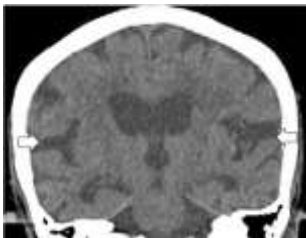

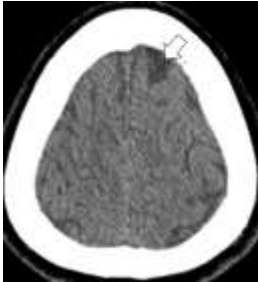




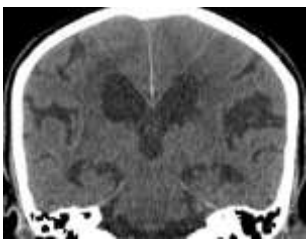
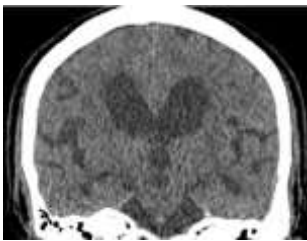
Seven radiological parameters were used in this study, including Evans' index, narrow sulci at high parietal convexity, dilatation of the Sylvian fissures, focally enlarged sulci, widening of temporal horns, callosal angle, and periventricular hypodensities. Each radiological parameter was separately converted into a point system with cut-off values based on earlier studies [3] and total scores were calculated, ranging from 0 to 12 points. The study also compared the reliability of each imaging feature alone with that of the overall iNPH Radscale score. To standardize measurements of each radiologic parameters, the planes were carefully aligned with anatomical landmarks in both axial and coronal planes. The axial plane was positioned parallel to the pituitary-fastigium (of the fourth

ventricle) axis, while the coronal plane was angulated perpendicular to the transverse plane for all measurements except for the callosal angle, which required a coronal plane perpendicular to the intercommissural plane [3].

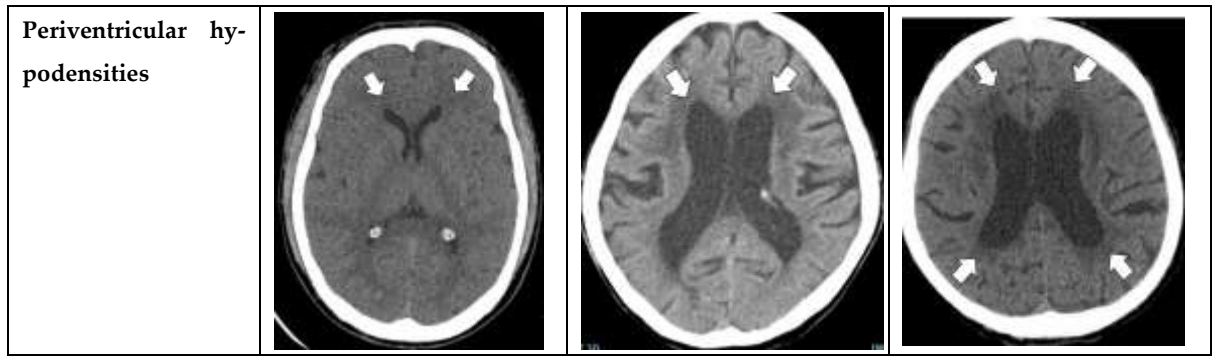
### **Radiologic parameters**

The following radiological parameters were evaluated by two radiologists and third year radiology resident. (Figure 1. for atlas of measurements and scoring levels [3])

- Evans' index: the ratio between the maximal width of the frontal horns of the lateral ventricles [B-C] by the maximal width of the inner table of the cranium in the same axial image [5].
- Narrow parietal sulci: at high-convexity and parafalcine region assessed in both axial plane in the most superior slices and coronal plane [6].
- Dilation of the Sylvian fissures: reported as present or not present in the coronal plane compared with surrounding sulci [7].
- Focally enlarged sulci: compared with surrounding sulci, usually found in coronal or axial planes [8].
- Temporal horns: reported as mean width of the right and left side, measuring in the axial plane [7].
- Callosal angle: angle between the lateral ventricles in the coronal plane through the posterior commissure perpendicular to the intercommissural plane [9].
- Periventricular hypodensities: along the lateral ventricles graded as not present, present as a cap around frontal horns or confluent extending around the lateral ventricles [10].

Radiologic markers	0	1	2
Evans' index			
Narrow sulci at high parietal convexity			
Dilatation of the Sylvian fissures			
Focally enlarged sulci			
Widening temporal horns			
Callosal angle			





**Figure 1.** Imaging atlas with scoring according to the NPH scale [3].

### AI evaluation

The study involved the segmentation from weakly supervised learning of 217 CT scans of all patients to extract features for NPH classification. The extracted features were classified into two categories, namely global features representing entire brain region characteristics and local features representing entire brain region characteristics. The study aimed to analyze the impact of both global whole-brain volume metrics and local partition-brain metrics on NPH classification.

The parameters for each feature in cerebrospinal fluid (CSF), White & Grey (WG) ratio, and standard deviation (Std) are shown below:

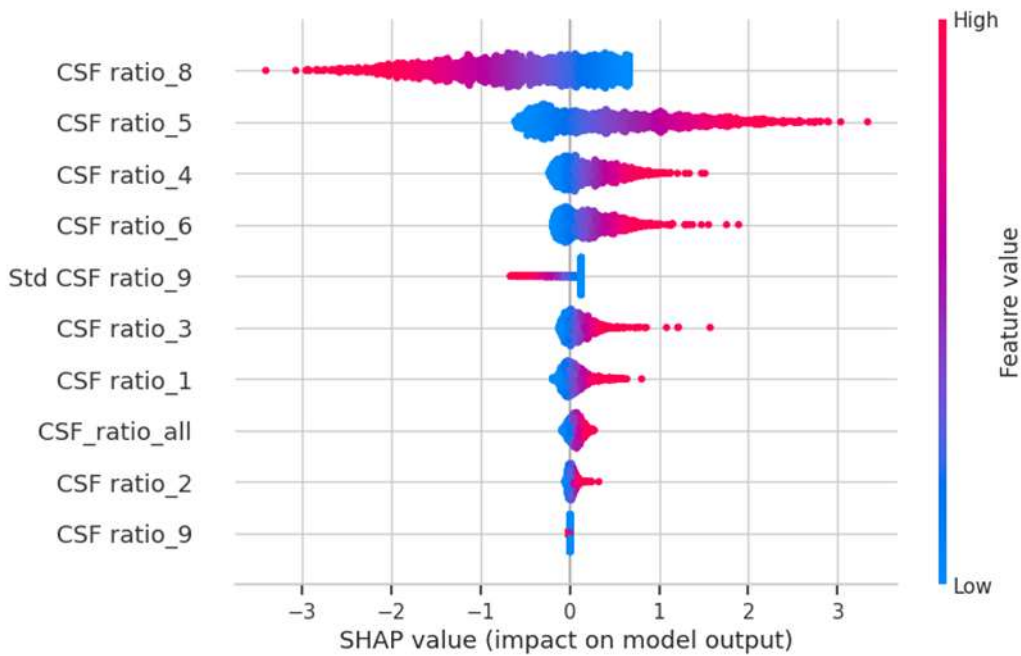
$$\begin{aligned}
 \text{CSF ratio all} &= \frac{N_{\text{CSF}}}{N_{\text{CSF}} + N_{\text{white\&grey}}} \\
 \text{CSF-WG ratio} &= \frac{N_{\text{CSF}}}{N_{\text{white\&grey}}} \\
 \text{CSF size} &= \frac{N_{\text{CSF}}}{\text{image\_size}} \\
 \text{Brain size} &= \frac{N_{\text{white\&grey}}}{\text{image\_size}} \\
 \text{Mean CSF ratio} &= \frac{\sum_{i=0}^n X_i}{n} ; X_i = \frac{N_{\text{CSF}}}{N_{\text{CSF}} + N_{\text{white\&grey}}} \\
 \text{Min CSF ratio} &= \text{Min of } \frac{N_{\text{CSF}}}{N_{\text{CSF}} + N_{\text{white\&grey}}} \\
 \text{Max CSF ratio} &= \text{Max of } \frac{N_{\text{CSF}}}{N_{\text{CSF}} + N_{\text{white\&grey}}} \\
 \text{Std CSF ratio} &= \sqrt{\frac{\sum |x - \bar{x}|^2}{n}} ; \bar{x} = \frac{N_{\text{CSF}}}{N_{\text{CSF}} + N_{\text{white\&grey}}} \\
 \text{Mean CSF-WG ratio} &= \frac{\sum_{i=0}^n X_i}{n} ; X_i = \frac{N_{\text{CSF}}}{N_{\text{white\&grey}}} \\
 \text{Min CSF-WG ratio} &= \text{Min of } \frac{N_{\text{CSF}}}{N_{\text{white\&grey}}} \\
 \text{Max CSF-WG ratio} &= \text{Max of } \frac{N_{\text{CSF}}}{N_{\text{white\&grey}}} \\
 \text{Std CSF-WG ratio} &= \sqrt{\frac{\sum |x - \bar{x}|^2}{n}} ; \bar{x} = \frac{N_{\text{CSF}}}{N_{\text{white\&grey}}}
 \end{aligned}$$

This evaluation utilizes  $N_{\text{CSF}}$  and  $N_{\text{white\&grey}}$  to represent the number of CSF and white/gray matter pixels within the segmentation masks. Meanwhile, *image\_size* indicates the overall number of pixels in a brain slice.

In the AI study, a logistic regression model was trained using 5-fold cross validation on 227 NPH and 110 normal data. The model was used a regularization parameter  $c=10$ , and feature selection was performed using the chi-square (chi2) method, resulting in the selection of 10 features: 'CSF\_ratio\_5', 'CSF\_ratio\_4', 'CSF\_ratio\_6', 'CSF\_ratio\_9', 'Std CSF\_ratio\_9', 'CSF\_ratio\_3', 'CSF\_ratio\_2', 'CSF\_ratio\_1', 'CSF\_ratio\_8', 'CSF\_ratio\_all'. The partitions 0-9 indicate different levels of the brain, with 0 being the lowest (closest to the neck) and 9 being the highest (at the top of the head).

To gain insights into the factors influencing our AI model's predictions, we leveraged the SHAP library [<https://github.com/slundberg/shap>] to assess the impact of each feature when predicting the NPH probability for each CT scan. Our analysis revealed that the

three most influential features were CSF ratio\_8, CSF ratio\_5, and CSF ratio\_4 (refer to Figure 2). CSF ratio\_8 captures changes in focal sulcal enlargement, while CSF ratio\_5 and CSF ratio\_4 correspond to enlarged ventricular regions (see Figure 3). This finding indicates that our AI model focuses on the key areas commonly examined by neuroradiologists during NPH diagnosis, underscoring its alignment with expert practices.



**Figure 2.** The SHAP values suggest that our AI model predictions were significantly influenced by the CSF ratio\_8, CSF ratio\_5, and CSF ratio\_4, which are regions that neuroradiologists commonly focus on during the diagnosis process.



**Figure 3.** Samples of brain slice images from partition 8, 5, and 4, arranged from left to right that visually demonstrate the specific brain regions associated with the CSF ratios that play a crucial role in NPH prediction.

Statistical analysis

Clinical data and radiological findings were presented with descriptive statistics. Categorical data were present as numbers and percentages and compared using Pearson’s Chi-square test. Continuous data were reported as mean ± standard deviation (SD) and compared using independent t-test. A p-value of <0.05 was considered statistically significant. Both the normal and NPH groups were compared to assess the sensitivity, specificity, accuracy, PPV, NPV, and area under the receiving operating characteristic (ROC) curve between radiologists and AI. A binary logistic regression was used to determine the cut-off value for predicting whether the patient was normal, borderline, or had NPH.

3. Results

This study retrospectively enrolled 217 subjects, including 112 patients clinically confirmed with NPH who underwent the gold standard CSF closing pressure-guided tap tes, and 105 normal patients. Among the NPH group, 108 patients were classified as iNPH, while only 4 patients are secondary NPH. The median age at the time of the clinical diagnosis was 76 years (range, 68–84 years); and 60 (57.1%) were men and 45 (42.9%) were women (Table 1). Clinical symptoms, including gait disturbance, urinary incontinence, and memory impairment are statistically significant ( $P<0.001$ ) in the NPH group (Table 1). Univariate and multivariate analyses found that four radiological parameters (Evans' index, dilated Sylvian fissures, focally enlarged sulci, widening temporal horns) were significantly associated with clinical symptoms with  $p$ -value  $< 0.0001$  (Table 2). Binary logistic regression analysis indicated that total scores of  $< 3$  points, 3-4 points, and  $\geq 5$  points were likely to be considered normal, borderline, or patients with NPH (Table 4).

The sensitivity for radiologists and AI was 77.14% and 99.05%, respectively, with a specificity of 98.21% and 57.14%, respectively, under the cut-off value of 5. NPV, PPV, and accuracy for radiologists were 82.09%, 97.59%, and 88.02%, respectively while for AI, these values were 98.46%, 68.42%, 77.42% respectively (Table 5). The receiver operating characteristic (ROC) curve of the diagnostic index of radiological parameters measured by radiologists for diagnosis of NPH (Figure 4) demonstrated an area under the curve of 0.954 ( $P<0.001$ ) and the ROC AI (Figure 5) was 0.784 ( $P<0.001$ ). Narrow sulci of high parietal convexity, callosal angle, and periventricular hypodensities are omitted due to collinearity.

The odds ratios (ORs) for Evans' index, dilated sylvian fissures, focally enlarged sulci, and widening temporal horns were found to be statistically significant. Multivariate analysis revealed ORs of 3.49 (1.07-11.42) and 38.37 (6.04-243.56) for Evans' index of 1 and 2, respectively. The OR for dilated Sylvian fissures was 3.07 (1.04-9.08), while for focally enlarged sulci was 7.88 (1.28-48.25), and for widening temporal horn was 5.35 (1.88-15.16) and 12.55 (2.15-73.31) for the 1st and 2nd grades, respectively (Table 2)

**Table 1.** Basic characteristics and demographic data between groups of normal and patients with NPH.

Variables	All (n = 217)	Normal (n = 112)	NPH (n = 105)	P-value
Gender (M: F)	105 (48.4%) : 112 (51.6%)	55 (49.1%):57 (50.9%)	60 (57.1%):45 (42.9%)	0.236
Age (years)	65.4 $\pm$ 17.8	55.7 $\pm$ 19.2	75.7 $\pm$ 8.0	<0.001
Gait disturbance	99 (45.6%)	0 (0%)	99 (94.3%)	<0.001
Urinary incontinence	77 (35.5%)	0 (0%)	77 (73.3%)	<0.001
Memory impairment	61 (28.1%)	0 (0%)	61 (58.1%)	<0.001
HT*	122 (56.2%)	49 (43.8%)	73 (69.5%)	<0.001
T2DM	72 (33.2%)	26 (23.2%)	46 (43.8%)	<0.001
DLP	80 (36.9%)	42 (37.5%)	38 (36.2%)	0.842
Old CVA	42 (19.4%)	21 (18.8%)	21 (20.0%)	0.816
CKD	21 (9.7%)	1 (0.9%)	10 (9.5%)	0.941
CAD	20 (9.2%)	8 (7.1%)	12 (11.4%)	0.275
Parkinson's disease	23 (10.6%)	0 (0%)	23 (21.9%)	<0.001
Dementia	20 (9.2%)	3 (2.7%)	17 (16.2%)	<0.001
OA knee	11 (5.1%)	6 (5.4%)	5 (4.8%)	0.842

\*HT, hypertension; T2DM, type 2 diabetes mellitus; DLP, dyslipidemia; Old CVA, old cerebrovascular accident; CKD, chronic kidney disease; CAD, coronary artery disease; OA knee, osteoarthritis of the knee

**Table 2.** Relationship of radiologic parameters to predict the likelihood of NPH.

Variable	<sup>1</sup> Crude OR* (95% CI)**	P value	<sup>2</sup> Adjusted OR (95% CI)	P value
----------	--------------------------------------	---------	--------------------------------------	---------



Evans' index		<0.0001	<0.0001
0	Ref.***		Ref.
1	12.77 (4.68-34.88)		3.49 (1.07-11.42)
2	395.3 (73.91-2114.10)		38.37 (6.04-243.56)
Dilatation of Sylvian fissures		<0.0001	<0.0001
0	Ref.		Ref.
1	23.25 (11.12-48.62)		3.07 (1.04-9.08)
Focally enlarged sulci		<0.0001	<0.0001
0	Ref.		Ref.
1	25.499 (0.762-85.30)		7.88 (1.28-48.25)
Widening temporal horns		<0.0001	<0.0001
0	Ref.		Ref.
1	30 (12.83-70.13)		5.35 (1.88-15.16)
2	132 (28.86-603.79)		12.55 (2.15-73.31)

\* OR, odds ratio; \*\*CI, confidence interval; \*\*\*Ref, reference  
<sup>1</sup> Univariate analysis by Pearson's Chi-Square, <sup>2</sup> Multivariate analysis

Table 3. Percentage of the total scores of radiologic parameters between normal and NPH groups

Total score	Normal	NPH	P-value
0	46 (100%)	0	< 0.0001
1	30 (96.8%)	1 (3.2%)	< 0.0001
2	15 (75%)	5 (25%)	0.028
3	12 (63.2%)	7 (36.8%)	0.292
4	7 (38.9%)	11 (61.1%)	0.259
5	1 (5.6%)	17 (94.4%)	< 0.0001
6	1 (5%)	19 (95%)	< 0.0001
7	0	19 (100%)	< 0.0001
8	0	11 (100%)	< 0.0001
9	0	9 (100%)	0.002
10	0	4 (100%)	0.037
11	0	2 (100%)	0.142
12	0	0	N/A

Table 4. Scoring levels used for NPH prediction.

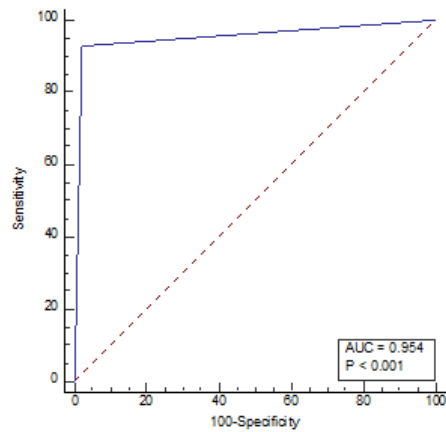
Score	Result of predicted NPH
0-2	Negative
3-4	Borderline
≥ 5	Positive

Table 5. Comparison of sensitivity, specificity, NPV, PPV, and accuracy between radiologists and AI using score ≥ 5 as the cut off value.

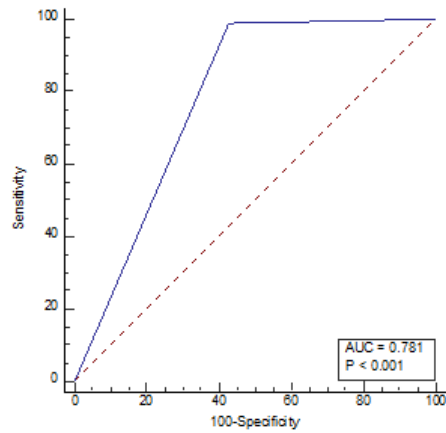
Variables	Radiologists	AI***
-----------	--------------	-------

Sensitivity	77.14%	99.05%
Specificity	98.21%	57.14%
NPV*	82.09%	98.46%
PPV**	97.59%	68.42%
accuracy	88.02%	77.42%

\*NPV, negative predictive value; \*\*PPV, positive predictive value.  
\*\*\*AI, artificial intelligence.



**Figure 4.** Receiver operating characteristic (ROC) curve of radiological parameters by radiologists.



**Figure 5.** Receiver operating characteristic (ROC) curve of AI.

#### 4. Discussion

The study findings suggest that NPH is increasingly being diagnosed in elderly patients undergoing brain imaging for other reasons. This is consistent with recent epidemiological surveys in Sweden that reported a 3.7% prevalence of iNPH among individuals aged 65 years old [11]. NPH is more likely to occur in the elderly and is often associated with other age-related diseases such as hypertension, T2DM, Parkinson's disease, and dementia [12]. The clinical symptoms included gait disturbance, urinary incontinence, and memory impairment are statistically significant ( $P < 0.001$ ) in the NPH group. It should be noted that our study mainly focused on iNPH cases due to the small number of secondary NPH.

Although various radiological parameters are used to help confirm the diagnosis, the cut-off values of each parameter are not well established. The morphologic features indicating the likelihood of morphologic features of NPH remain undefined. Furthermore, NPH commonly affects the elderly who may have associated age-related brain atrophy. Therefore, the differential diagnosis between iNPH and cortical brain atrophy or small vessel disease are difficult [13]. Our study investigated the radiologic parameters in both NPH and normal groups of patients and compared results found in AI.

There is no united agreement in standardized measurement for each radiologic parameter. For example, there are no specific images used in the measurements of Evans' index which is the most widely used parameter in ventricular width. Because CT of the brain provides numerous axial images, the maximal width of the frontal horns can be measured on the same or different images by each radiologist [14]. Besides, some radiologists measure the maximal width of the frontal horns and maximal inner diameter on the same axial image [15], while some measure maximal width in the separate planes [16]. Temporal width in our study is assessed in the axial plane and reported as mean width of the right and left side [7]. Measurement of its values may differ depending on the selection of images by each radiologist. Some of the radiologic parameters such as narrow sulci at high parietal convexity, dilatation of the Sylvian fissures, focally enlarged sulci, and periventricular hypodensities are evaluated by using subjective methods namely the visual rating score [17]. Dilated Sylvian fissures and focally enlarged sulci are frequently misinterpreted for cerebral atrophy [8]. However, the interobserver analysis was consistent in our study. The assessment of the callosal angle ideally should be measured on a coronal image perpendicular to anterior commissure – posterior commissure (AC-PC) plane at the level of the posterior commissure. However, minor difference in angular malrotations of the true coronal plane could affect accurate measurement of callosal angle [18].

Although periventricular hypodensities are a supporting feature of NPH, it is difficult to separate between white matter ischemia which is commonly found in elderly patients with small vascular disease and subependymal effusion resulting from NPH and results in exclude patients from further NPH evaluation [19]. It can be seen that radiological parameters performed by different methods may have the different results [20]. Nowadays, volumetric segmentation of CT brain scan methods are considered more accurate and are increasingly used in many studies [21-22].

Zhang et al. propose an automated method of predicting NPH using volumetric segmentation of CT brain scans which is the first method which automatically predicts NPH from CT scans for prediction by AI. The connectome data to compute features which capture the impact of enlarged ventricles and regions of interest segmented from CT scans using AI provide the fast and accurate volumetric segmentation of CT brain scans which can improve the NPH diagnosis accuracy [23].

Our study found that radiologists had better diagnostic specificity, PPV, and overall accuracy than AI. However, AI volumetric segmentation demonstrated higher sensitivity in detecting ventricular enlargement, indicating its potential as a screening tool. Moreover, the accuracy of AI can be improved through a learning process that involves

measuring brain volumes in an increasing number of patients. As AI technology continues to advance, it may become a valuable tool for diagnosing and managing NPH.

## 5. Limitation

As our study is a retrospective review of 10 years' worth of data, there is a risk of chronological bias. Furthermore, certain radiological parameters such as narrow sulci at the high parietal convexity, callosal angle, and periventricular hypodensities were omitted due to collinearity. Therefore, a large-scale prospective study is needed to further investigate these parameters and confirm our findings.

## 6. Conclusions

Our study found that radiologists exhibited higher diagnostic sensitivity, specificity, PPV, and accuracy than AI. However, AI can serve as a screening tool in patients suspected of having NPH, reducing the workload on radiologists. Furthermore, AI's accuracy can be enhanced through machine learning on an increasing number of brain volumetric measurements. In the future, AI may attain capabilities that are equivalent to or surpass those of radiologists in diagnosing hydrocephalus.

**Author Contributions:** Writing—review and editing, methodology, investigation, D.S.; writing—first draft, investigation, formal analysis, P.N.; data curation, methodology, J.W.; resources, software and validation, S.K.; resources, software and validation, P.A.; formal analysis, project administration, P.P.; supervision, validation, writing—review and editing, A.S.

**Funding:** This research received no external funding.

**Institutional Review Board Statement:** The study was approved by the Institutional Review Board of Faculty of Medicine Siriraj Hospital, Mahidol University (certificate of approval(COA) MU-MOU 671/2022 on 13 September 2022).

**Acknowledgments:** The authors would like to thank Dollaporn Polyeam and Karnchana sae-jang from Department of Radiology, Faculty of Medicine Siriraj Hospital for their assistance with the statistical analysis.

**Conflicts of Interest:** The authors declare no conflict of interest.

## References

1. Damasceno BP. Neuroimaging in normal pressure hydrocephalus. *Dement Neuropsychol.* 2015;9(4):350-355.
2. Kockum K, Virhammar J, Riklund K, Söderström L, Larsson EM, Laurell K. Standardized image evaluation in patients with idiopathic normal pressure hydrocephalus: consistency and reproducibility. *Neuroradiology.* 2019;61(12):1397-1406.
3. Kockum K, Lilja-Lund O, Larsson E et al. The Idiopathic Normal-Pressure Hydrocephalus Radscale: A Radiological Scale for Structured Evaluation. *Eur J Neurol.* 2018;25(3):569-76.
4. Zhou X, Ye Q, Yang X, et al. AI-based medical e-diagnosis for fast and automatic ventricular volume measurement in patients with normal pressure hydrocephalus [published online ahead of print, 2022 Feb 24]. *Neural Comput Appl.* 2022;1-10.
5. Evans WJ. An encephalographic ratio for estimating ventricular enlargement and cerebral atrophy. *Arch Neuropsych.* 1942;47(6):931-937.
6. Sasaki M, Honda S, Yuasa T, Iwamura A, Shibata E, Ohba H. Narrow CSF space at high convexity and high midline areas in idiopathic normal pressure hydrocephalus detected by axial and coronal MRI. *Neuroradiology.* 2008;50(2):117-122.
7. Virhammar J, Laurell K, Cesarini KG, Larsson EM. Preoperative prognostic value of MRI findings in 108 patients with idiopathic normal pressure hydrocephalus. *AJNR Am J Neuroradiol.* 2014;35(12):2311-2318.
8. Holodny AI, George AE, de Leon MJ, Golomb J, Kalnin AJ, Cooper PR. Focal dilation and paradoxical collapse of cortical fissures and sulci in patients with normal-pressure hydrocephalus. *J Neurosurg.* 1998;89(5):742-747.
9. Ishii K, Kanda T, Harada A, et al. Clinical impact of the callosal angle in the diagnosis of idiopathic normal pressure hydrocephalus. *Eur Radiol.* 2008;18(11):2678-2683.
10. Fazekas F, Chawluk JB, Alavi A, Hurtig HI, Zimmerman RA. MR signal abnormalities at 1.5 T in Alzheimer's dementia and normal aging. *AJR Am J Roentgenol.* 1987;149(2):351-356.
11. Andersson J, Rosell M, Kockum K, Lilja-Lund O, Söderström L, Laurell K. Prevalence of idiopathic normal pressure hydrocephalus: A prospective, population-based study. *PLoS One.* 2019;14(5):e0217705.

12. Oliveira LM, Nitrini R, Román GC. Normal-pressure hydrocephalus: A critical review [published correction appears in Dement Neuropsychol. 2019 Jul-Sep;13(3):361]. Dement Neuropsychol. 2019;13(2):133-143.
13. Maytal J, Alvarez LA, Elkin CM et-al. External hydrocephalus: radiologic spectrum and differentiation from cerebral atrophy. AJR Am J Roentgenol. 1987;148 (6): 1223-30.
14. Toma A. K., Holl E., Kitchen N. D., Watkins L. D. (2011). Evans' index revisited: the need for an alternative in normal pressure hydrocephalus. Neurosurgery. 68, 939–944. 10.1227
15. Del B. O., Mera R. M., Gladstone D., Sarmiento-Bobadilla M., Cagino K., Zambrano M., et al.. (2018). Inverse relationship between the evans index and cognitive performance in non-disabled, stroke-free, community-dwelling older adults. A population-based study. Clin Neurol Neurosurg. 169, 139–143. 10.1016
16. Ambarki K, Israelsson H, Wåhlin A, Birgander R, Eklund A, Malm J. Brain ventricular size in healthy elderly: comparison between Evans index and volume measurement. Neurosurgery. 2010;67(1):94-99.
17. Narita W, Nishio Y, Baba T, et al. High-Convexity Tightness Predicts the Shunt Response in Idiopathic Normal Pressure Hydrocephalus. AJNR Am J Neuroradiol. 2016;37(10):1831-1837.
18. Lee W, Lee A, Li H, et al. Callosal angle in idiopathic normal pressure hydrocephalus: small angular mal-rotations of the coronal plane affect measurement reliability. Neuroradiology. 2021;63(10):1659-1667.
19. Tullberg M, Jensen C, Ekholm S, Wikkelsø C. Normal pressure hydrocephalus: vascular white matter changes on MRI must not exclude patients from shunt surgery. Am J Neuroradiol. 2001;22:1665–1673.
20. Zhou X, Xia J. Application of Evans Index in Normal Pressure Hydrocephalus Patients: A Mini Review. Front Aging Neurosci. 2022;13:783092.
21. Wu D, Moghekar A, Shi W, Blitz AM, Mori S. Systematic volumetric analysis predicts response to CSF drainage and outcome to shunt surgery in idiopathic normal pressure hydrocephalus. Eur Radiol. 2021;31(7):4972-4980.
22. Muscas, G, Matteuzzi, T, Becattini, E, et al. Development of machine learning models to prognosticate chronic shunt-dependent hydrocephalus after aneurysmal subarachnoid hemorrhage. Acta neurochirurgica, 2022;162:3093-3105.
23. Zhang A, Khan A, Majeti S, Pham J, Nguyen C, Tran P, et al. Automated Segmentation and Connectivity Analysis for Normal Pressure Hydrocephalus. BME Frontiers 2022;2022:1-13.